ACTA IMEKO
ISSN: 2221-870X
June 2025, Volume 14, Number 2, 1 – 9

Phasor measurement units' responsiveness: Fault simulations in a 5G network environment

Alberto Morato[1], Guglielmo Frigo[2], Federico Tramarin[3]

[1] *National Research Council of Italy CNR-IEIIT, Padova, Italy, alberto.morato@cnr.it*
[2] *Federal Institute of Metrology Electrical Energy and Power Lab, Bern-Wabern, Switzerland, guglielmo.frigo@metas.ch*
[3] *University of Modena and Reggio Emilia Dept. of Engineering "Enzo Ferrari", Modena, Italy, federico.tramarin@unimore.it*

ABSTRACT
In the era of electrical substation digitalization, the reliability of Phasor Measurement Units (PMUs) is crucial. This paper addresses the impact of fault conditions in PMUs on system reaction time in a 5G network environment. We focus on fault-critical conditions in communication systems, particularly in the presence of PMU-based measurement systems. We perform a series of simulations to evaluate the performance of the 5G infrastructure for transmitting IEC61850 data. Results from simulations show that the performance in terms of latency and packet loss is strongly influenced by the topology of 5G networks, particularly the number and deployment of gNBs (5G base stations) serving PMU systems. The analysis of the two case studies underscores the importance of considering the specific characteristics of each fault event when designing and deploying PMU/PDC systems capable of real-time fault detection and response, ensuring the stability and reliability of the power grid. This will involve simulating various fault scenarios and communication network impairments to better understand their impact on the overall system performance and to mitigation strategies to improve the reliability and resilience of the PMU system in real-world deployment scenarios.

Section: RESEARCH PAPER

Keywords: Digital substation; IEC 61850; 5G communication; phasor measurement unit; transmission latency

Citation: A. Morato, G. Frigo, F. Tramarin, Phasor measurement units' responsiveness: Fault simulations in a 5G network environment, Acta IMEKO, vol. 14 (2025) no. 2, pp. 1 – 9, DOI: 10.21014/actaimeko.v14i2.2068

Section Editor: Luca Callegaro, INRiM, Italy

Received: February 3, 2025; **In Final Form:** June 25, 2025; **Published:** June, 2025.

Funding: This research has been supported in part within the activities of the project "Time Sensitive Networking for future enabling technologies: measurement methods and metrological characterization in hybrid wired/wireless scenarios" — CUP E53D23014650001, funded by EU in NextGenerationEU plan through the Italian "Bando Prin 2022 PNRR - D.D. 1409 del 14-09-2022" by MUR.
This research has been also carried out within the PNRR research activities of the consortium iNEST (Interconnected North-Est Innovation Ecosystem) funded by the European Union Next-GenerationEU (Piano Nazionale di Ripresa e Resilienza (PNRR) - Missione 4 Componente 2, Investimento 1.5 - D.D. 1058 23/06/2022, ECS_00000043)

Corresponding Author: Alberto Morato, e-mail: alberto.morato@cnr.it

1. INTRODUCTION

The rapid adoption of distributed generation and renewable energy sources is driving a significant transformation in modern power networks [1], [2]. Electrical substations are increasingly shifting towards fully digital architectures, including advanced measurement and communication infrastructures [3], [4]. Within this framework, the IEC 61850 standard [5] presents the performance criteria and communication protocols for the various equipment and functions found in a digital substation [6]–[8]. It provides a number of communication types, such as protocols for Generic Object Oriented Substation Events (GOOSE) and Sampled Value (SV). To facilitate a more seamless transition and increased interoperability, it can also utilize existing data formats, such as those used by measuring instruments today. Phasor Measurement Units (PMUs) play a crucial role in this digital ecosystem, generating time-synchronized measurement data packets, typically transmitted via Ethernet using TCP or UDP protocols. These data streams support real-time monitoring and control routines, essential for managing the variability of renewable energy sources. However, achieving a balance between scalability, financial feasibility, and system responsiveness presents unique challenges [9]. Different and conflicting requirements in this circumstance must be appropriately matched. A quick and capillary monitoring system that can handle several devices and report at tens of frames per second is required due to the unstable nature of renewable energy sources [10], [11]. However, it is not always feas-

ible or financially sustainable to realize a completely connected system [12], [13]. To solve this, recent research has examined the viability and potential benefits of applying 5G mobile communication technologies in power systems, particularly in distribution grids with short substation-to-substation distances where a single or small number of antennas can adequately cover the whole region of interest [14]–[16]. In this context, it is important to understand the traffic profile in normal and faulty operating conditions. For this analysis, we consider the measurement packets are produced by Phasor Measurement Units (PMUs), since this class of instruments is widely employed for many monitoring and control routines [1], [2], [17], [18]. In such applications, though, latency plays a crucial role and it is important to characterize each contribution that may affect the overall control system responsiveness [19], [11]. To this end, the contribution of the communication infrastructure cannot be neglected, especially when affected by technical faults and resources' limitations [20]–[22].

In this paper, we address this problem by means of a numerical analysis. Basically, we extend [23] considering a real-world distribution network with 18 buses, already used as a test-bench for similar analysis. We characterize the statistical distributions of packet losses and transmission latencies in the presence of several PMUs synchronized to the same time reference. With respect to the conference proceedings paper, we clarify the theoretical background of the numerically simulated scenario, and we discuss how the parameter setting may affect the final results. We also evaluate the validity and the significance of the obtained results in two realistic scenarios, as inspired by the recent literature of power system contingencies. To this end, we reproduce a plausible stream of measurements related to two faults in real-world transmission networks, such as the 2016 blackout in South Australia and the 2011 Southwest blackout in the United States. For this analysis, we consider measurements as output by Phasor Measurement Units (PMUs), which are the most accurate and responsive devices currently deployed in power systems. In a conservative approach, we characterize the worst-case latency of frequency and ROCOF measurements when both the estimation latency, and the transmission latency are considered. Moreover, we consider possible issues that may arise in a real-world scenario. On one side, the loss of the synchronization source (e.g., the loss of GPS signal) at PMU level. On the other side, an error in the transmission protocol that produces additive random delays in the PMU measurement stream. The cumulative effect of all these contributions repesent a significant benchmark for the validation of time-sensitive applications as the ones related to the monitoring and control of large power systems.

This paper is structured as follows: Section 2. details the simulation setup, including the 5G network model and fault scenarios. Section 3. discusses the results, emphasizing latency and packet loss under varying configurations. Section 4. focuses on the ability of 5G-enabled PMUs to detect and respond to grid faults. Finally, Section 5. provides concluding remarks and outlines future research directions.

2. SIMULATION SETUP

In this section we describe the simulation model and parameters to reproduce the 5G communication infrastructure to serve the power grid.

2.1. Power grid and 5G network

In our analysis, we focus on a 10-kV three-phase distribution network situated in the Netherlands and operated by DSO Alliander.

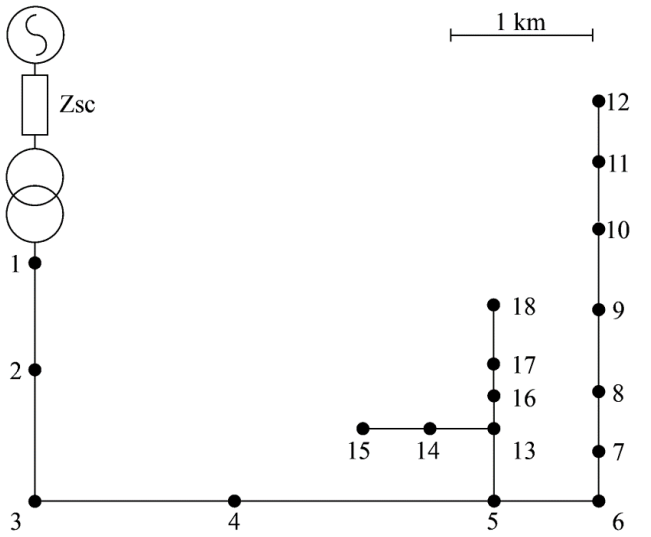

Figure 1. 18-bus distribution feeder located in the Netherlands and operated by Alliander.

The network's architecture is detailed in Figure 1, where it is illustrated that the system consists of 18 nodes, each equipped with a Phasor Measurement Unit (PMU). In our simulation scenario, we postulate that the Phasor Data Concentrator is located at Node 1, with all PMUs functioning at a consistent reporting rate of 50 frames per second (fps). Nonetheless, our simulation also takes into account potential drift within the PMUs' internal clocks, causing each PMU to produce a frame roughly every 20 milliseconds, with a variability of ±100 nanoseconds. This hypothetical scenario facilitates a more accurate and realistic simulation of the true latencies and packet loss that may occur. Despite the fact that clock drift can pose difficulties, potentially threatening measurement accuracy, it might also provide benefits during the communication process. In essence, transmissions that are slightly skewed and unsynchronized can diminish the probability of collisions when attempting to access the transmission medium, along with decreasing the instant peak bandwidth utilization across the network. Consequently, this could lead to advancements regarding latency and packet loss, thereby significantly increasing the overall efficiency and performance of the system. The chosen distribution network offers intriguing insights into the strategic positioning of gNBs for the accommodation of PMUs. Given the relatively short line lengths, where none exceed 2 km and the average is approximately 0.5 km, it is significant to note that these distances are well-aligned with the optimal inter-gNB and UE-gNB distances observed in typical 5G scenarios, which vary from 0.1 km to 10 km. Consequently, it is clear that the inter-PMU distances in this scenario are entirely compatible with the standard requirements for 5G networks. In theory, it would be plausible to encompass all nodes within a single 5G network framework, employing one gNB alongside a coherent 5G RAN and backhaul network. However, while it is indeed feasible to manage the complete infrastructure within a solitary RAN, utilizing one gNB for connecting all PMUs (or all UEs) may present several challenges. Despite the capability of the backhaul network to handle bandwidths of several Gbps, the concentration of multiple PMUs' data to a single gNB could place considerable demands on the communication system, particularly in scenarios where numerous PMUs are transmitting concurrently. Additionally, deploying only a single gNB would result in an increased average UE-gNB distance, which can lead to a decrease in the signal-to-noise ratio (SNR), thereby compromising communication quality and

resulting in an increased likelihood of packet loss. It becomes apparent that, especially in applications within safety-critical contexts—such as the application discussed, where swift and timely fault responses are crucial—optimizing the network to reduce packet loss and latency is of utmost importance. In this regard, this study examines how varying configurations within the communication infrastructure impact packet loss and mean latency across different nodes. In the research conducted by [25], an identical network setup was utilized to evaluate the transmission of ten PMU measurement packets through a sequence of specialized 4G routers (R-1300, Garderos GmbH, Munich, Germany), which were subsequently connected to the Vodafone network without any implemented service level (thereby ensuring no prioritization of PMU traffic). In that setup, the latency exhibited a bimodal distribution with a central tendency around 70 ms. Conversely, packet loss is heavily contingent upon the policy deployed within the PDC [26]. The performance of the 5G communication infrastructure has been investigated through an appropriate simulation environment developed using the well-known OMNeT++ simulator, alongside its extension, the Simu5G framework [27], [28]. The model for both the protocol stack and transmission channel is based on specifications outlined in 3GPP Release 16 [29] .

2.2. Simulation parameters and communication infrastructure model

The distribution network that serves as the testbed is illustrated in Figure 1. At each black dot, a Phasor Measurement Unit (PMU) is installed to acquire data from the grid at that specific node. To simulate the testbed environment, the Simu5G framework was employed within the OMNeT++ simulator. In this setup, User Devices (UDs) gather measurement information, which they then relay through the 5G base station (gNB) network.

For communication to be efficient and effective, it is essential that 5G base stations (gNBs) are strategically positioned to service the maximum possible number of UDs while maintaining high-quality communication standards. The determination of gNB placements was accomplished through an optimization method, specifically the k-means algorithm. According to this algorithm, gNBs are situated in regions with a higher density of UDs. This density-centric placement strategy is depicted in Figure 2, which presents an example of clustering with four gNBs. By minimizing the average distance between UDs and the nearest gNBs, this approach enables the gNBs to be located closer to areas where there is a significant concentration of UDs. This optimized positioning enhances communication effectiveness and reduces packet loss. Furthermore, economic factors must also be considered because deploying a vast number of gNBs would neither be practical nor economically viable.

In our simulations, we utilized the User Datagram Protocol (UDP) as the transport protocol due to its connection-less nature. This means that any packet that is lost or malformed will not be retransmitted. In our design setup, the primary substation, designated as UD[0], acquires data from Phasor Measurement Units (PMUs) within an "Edge-to-Edge (E2E)" configuration that we have implemented. This configuration encompasses a backhaul network that is typically considered wired, although despite being wired, it can still somewhat contribute to the overall packet loss. To effectively simulate a scenario with a high density of gNodeBs (gNBs), we employed the 3GPP Technical Report (TR) 38.901 channel model which is designed for urban microcell environments. This model accounts for a variety of factors including interference, signal fading, and shadowing effects. Our simulations are conducted at a carrier frequency of 2 GHz. Additionally, we incorporate Adaptive Modulation and Coding (AMC) to adaptively tune the coding rate and modulation scheme based on the prevailing channel conditions. This approach is intended to reduce latency, enhance reliability, and increase the spectral efficiency of the system.

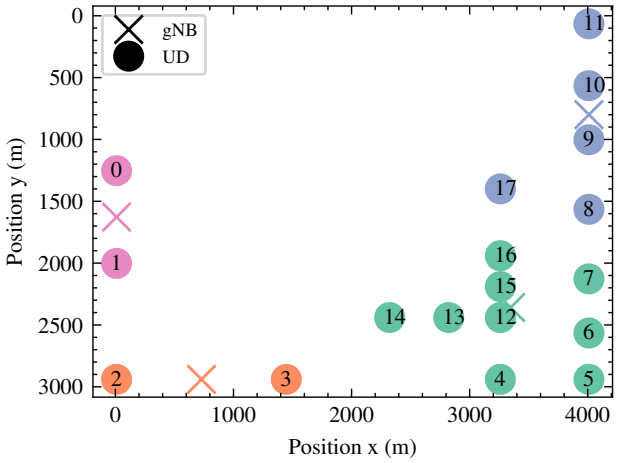

Figure 2. Position of the devices and gNBs in the simulated network with 4 gNBs. Circles represent the UDs i.e. the PMUs. Stars represent the position gNBs according to the k-means algorithm. The hue represents the number of clusters. Each device is connected to the gNB with the same colour.

We consider a scenario where a private 5G network is utilized to host the Phasor Measurement Units (PMUs) system. This notion is supported by the 3GPP Rel. 16 standard, which is focused on the implementation of Mobile Private Networks (MPNs) to develop highly reliable, dedicated networks. In this context, private networks can be implemented through two primary methods. The first approach, which is more reliable but also more costly, involves deploying a fully private 5G network where the operator has complete control over all systems, hardware, and private clouds. In contrast, a more conventional strategy employs network slicing functionalities to allocate bandwidth specifically within the public 5G network.

Table 1. Parameters used for the simulations.

Parameter	Value
Packet size	44 (bytes) according to IEEE C37.118.2
Simulation time	900 s
Packet generation frequency	50 pkt/s
Transmission typology	5G ULL
Channel model	3GPP TR 38.901 Channel Model for urban micro cell
Carrier frequency	2 GHz
UD Tx power	26 dBm
gNB Tx power	46 dBm
Inter-packet jitter	Uniform [-100, 100] ns
Transmission start delay	Uniform [0, 20] ms

In our simulation, we hypothesize the absence of any conflicting traffic. The inclusion of a more comprehensive analysis of specific traffic patterns and densities of interfering nodes is deferred to future investigations. Previously noted, to tackle possible issues due to temporal drifts within the PMUs' internal clocks, our simulation has been adjusted to introduce a consistent jitter of ±100 nanoseconds in the packet transmission rate at each node. Furthermore, to account for potential delays in connecting to the 5G network or discrepancies in the startup duration among the PMUs, we have integrated a random startup delay ranging from 0 to 20 milliseconds. This means the initial frame transmission from each PMU is postponed by this particular delay period. Beyond these factors, the simulation of the 5G network is performed with

the specific parameters that are detailed in Table 1.

3. ANALYSIS OF LATENCY AND PACKET LOSS IN THE 5G NETWORK

In this section, we conduct an in-depth examination of the outcomes related to packet loss and transmission latency. Our analysis specifically focuses on measuring latency and packet loss for each position of the gNBs, which were determined using the k-means clustering algorithm. When addressing latency, our emphasis is on End-to-End latency. This metric covers the total time taken from the moment a packet is transmitted from a Phasor Measurement Unit (PMU) to when it is received by a Phasor Data Concentrator (PDC), denoted in this context as UD[0]. It is crucial to note that this scenario represents a worst-case scenario, given that the latency involves traversing one or multiple 5G connections depending on whether the PMU and PDC are linked to different gNBs. Additionally, the End-to-End latency incorporates several Radio Access Network (RAN) latencies due to data transmission across the 5G network and includes any delays caused by the backhaul network, which is responsible for connecting the gNBs to the central server.

In relation to packet loss, we calculated the Packet Delivery Ratio (PDR), which is defined as the proportion of packets that are successfully delivered compared to the total number of packets sent, with the result expressed as a percentage. This metric provides valuable insights into the network's capability to reliably deliver packets, which is especially crucial when it comes to transmitting safety-critical information, such as data related to faults within the distribution network. By examining the PDR data as shown in Table 2, it becomes apparent that an increase in the number of gNBs leads to considerable improvements in the overall PDR. However, the maximum PDR is not consistently achieved in situations where only one or two gNBs are tasked with servicing the entire infrastructure. Although these scenarios culminate in similar packet loss outcomes, the underlying causes are distinctly different. For instance, when only a single gNB is present, the main reason for packet loss is the lack of a stable connection between the User Device (UD) and the gNB. Our observations indicate that in densely populated regions, particularly during the initial stages of network communication, such as joining the network and forming a connection with the nearest gNB, certain UDs may face challenges due to the high density of nodes attempting to join the network within a short window of time. Some nodes may be unable to join the network at all, while others might encounter delays during the network joining process. As a result, this situation leads to notable packet loss, since the application level expects that all packets will be successfully delivered, and the absence of connectivity means those packets are marked as lost.

In scenarios where two gNBs are used, a distinct situation arises compared to those with a greater number of gNBs. In this particular simulation, all User Devices (UDs) achieve connectivity; however, the substantial exchange of data results in some frame losses. In contrast, simulations deploying more than two gNBs experience minimal packet loss, if any. These observations highlight the pivotal role that the number of gNBs plays in networking, underscoring the necessity for deliberate network design to ensure each node receives sufficient coverage. This finding also implies that the ratio of UDs per gNB warrants significant consideration, as it is crucial for maintaining consistent connectivity. This aspect becomes particularly pertinent when planning for network expansions or increases in the number of UDs in future distributions. Regarding latency, Figure 3 illustrates the results, while an extensive breakdown is provided in Table 2. An examination

Table 2. Performance metrics for different gNBs.

gNBs	Mean (ms)	Std (ms)	Min (ms)	Max (ms)	PDR (%)
1	17.69	2.79	13.07	20.23	53.07
2	17.35	2.75	13.21	20.69	94.12
3	16.43	3.00	13.00	22.19	100.00
4	15.50	2.43	13.14	19.85	100.00
5	14.49	1.73	13.03	19.40	100.00
6	14.12	0.99	13.04	18.20	100.00
7	13.59	0.49	13.03	14.85	100.00
8	14.33	0.95	13.05	16.87	100.00
9	14.26	1.17	13.08	17.87	100.00
10	13.78	0.60	13.05	14.95	100.00
11	14.05	0.97	13.04	16.57	100.00
12	13.84	0.61	13.03	14.96	100.00
13	14.32	1.16	13.03	17.28	100.00
14	13.87	0.60	13.03	14.94	100.00
15	13.56	0.48	13.04	14.87	100.00

of the average latency values indicates a slight enhancement in latency and its standard deviation with a rise in the number of gNBs. Nevertheless, beyond five gNBs, there is no noteworthy improvement in latency, suggesting there exists an optimal range of gNBs that achieves the desired improvements in latency and reliability. Exceeding this range could result in diminishing returns and may impose superfluous infrastructure expenses. Thus, determining the correct number of gNBs is vital for the PMU-based distributed measurement system to attain set performance objectives, while also considering cost implications associated with implementing and sustaining the 5G technology. The behavior of maximum latency values reveals intriguing trends. As outlined in Figure 3 and detailed in Table 2, maximum latency increases with one, two, and three gNBs, contradicting the trend observed with mean latency values. Despite appearing counterintuitive, this increment is linked to the packet loss previously mentioned. With a higher number of gNB connections (corresponding to increased traffic), maximum latency spikes, prompted by potential moments of heightened instantaneous bandwidth demand, causing packet delays. The trajectory of maximum latency appears positive, echoing the trend seen with the Packet Delivery Ratio (PDR). However, from the point of introducing four gNBs, the trend shifts, and maximum latency begins to decline. In this particular setting, the network's bandwidth capacity adequately supports larger packet volumes as traffic spreads across various gNBs, thereby reducing maximum latency. This conclusion corroborates earlier findings regarding the optimal gNB count, accentuating the necessity for network designs capable of managing significant traffic bursts.

In this study, we expanded our examination of the intricate interactions among latency, the number of gNBs deployed, and the geographical distance between User Devices (UDs) and gNBs. The outcomes of this detailed analysis are depicted within Figure 4 and Figure 5. Figure 4 portrays the connection between latency and proximity to the nearest gNB, while Figure 5 illustrates the correlation between latency and the overall count of deployed gNBs.

The data presented in Figure 4 suggest that there exists no straightforward correlation between the latency experienced and the spatial separation from a gNB. This lack of a direct relationship highlights that the causes behind latency variations are not significantly tied to transmission medium conditions, such as Signal-to-Noise Ratio (SNR). Regardless of the specific User Device being assessed or its relative distance to the gNB, the patterns observed remain inconsistent and do not adhere to any

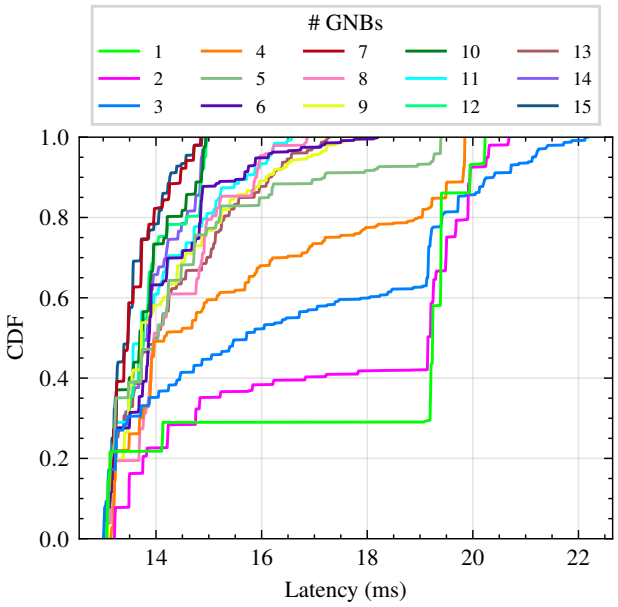

Figure 3. Cumulative Distribution Function of the communication delay, changing the number of gNBs.

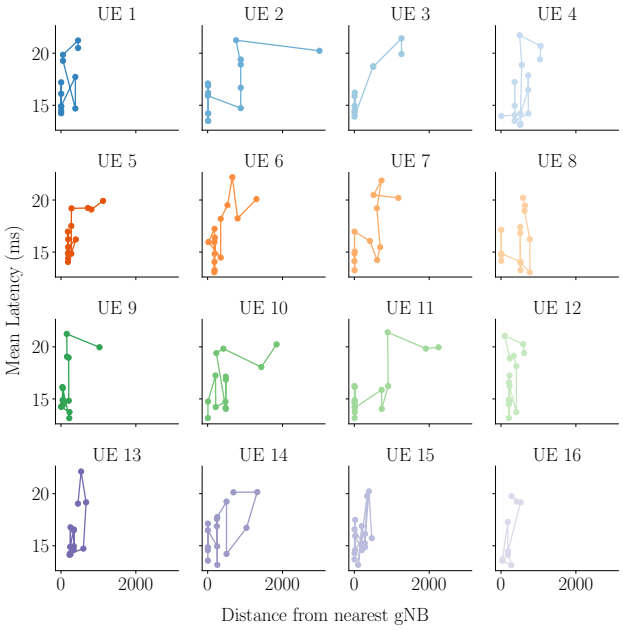

Figure 4. Mean latency over the distance from the nearest gNB for each UD.

discernible regular trend.

Conversely, Figure 5 demonstrates a quasi-linear association between the average latency and the quantity of gNBs in operation. This suggests that a principal source of latency appears to stem from traffic congestion, which arises due to the high volume of user connections, as opposed to being caused by channel conditions. This discernment further supports the perspective that latency is largely dictated by congestion factors within the communications framework. With the deployment of additional gNBs, network traffic becomes distributed more effectively across a wider array of unique pathways, thereby diminishing the probability of congestion occurrences.

The assessment of the applicability of 5G communication and its robustness against faults in Phasor Measurement Unit (PMU)-based measurement systems uncovers considerable benefits. As demonstrated, the utilization of the 5G Ultra Low Latency (ULL) profile facilitates deterministic and lossless communication under a variety of operational circumstances. Particularly, when a fault is communicated to the Phasor Data Concentrator (PDC) by the PMU, employing a 5G connection enables a significantly faster response time in comparison to a 4G connection, which generally results in delays spanning several hundred milliseconds.

Furthermore, the minimal variability, or jitter, within latency enables precise and timely fault identification within the PMU, including the detection of synchronization losses. Discrepancies in packet arrival rates at the PDC that exceed the typical communication jitter may signal potential synchronization losses within the PMU. Assuming the communication infrastructure remains consistent, the detection of sustained delays or notable deviations from the anticipated reporting rate becomes possible. This allows for the isolation of network-induced effects and the identification of potential synchronization discrepancies within the PMU.

Moreover, these considerations with respect to latency allow for rapid identification of packet loss occurrences. As demonstrated, the low variability in latency facilitates the definition of strict deadlines for packet reception. When such deadlines are exceeded, packets can be confidently considered lost. Within the examined scenario that features a reporting rate of 50 frames per second, all outlined fault conditions can be detected within the specific reporting interval, assuming that latency does not surpass

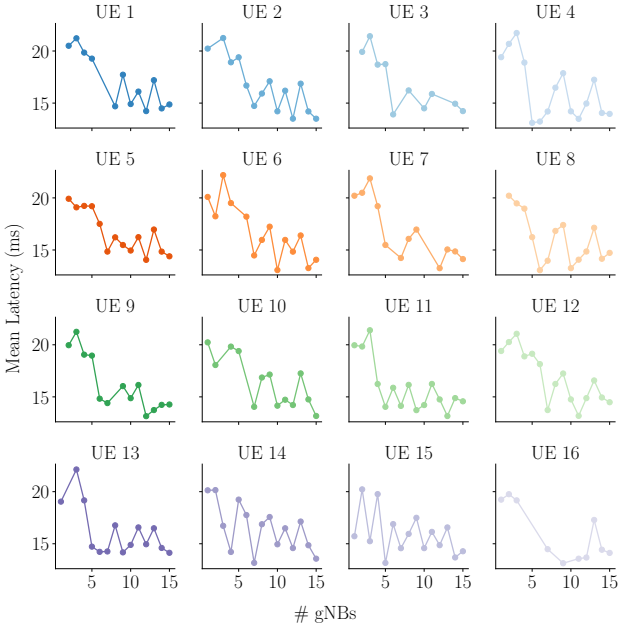

Figure 5. Mean latency over the total number of gNBs for each UD.

the reporting timeframe in most instances. This capability ensures swift reaction times and substantially augments the overall reliability of the system.

4. DETECTION AND RESPONSE TO POWER GRID FAULTS USING 5G-ENABLED PMUS

So far, we have focused on whether the 5G network can effectively transmit data from PMUs to the PDC and its potential for detecting synchronization faults or packet loss in the PMUs themselves. In this section, we shift our focus to the ability of 5G-enabled PMUs to detect and respond promptly to faults in the power grid.

Power grid faults can manifest in various forms, including frequency and voltage deviations that destabilize the grid when they significantly stray from the target operational range. Transformer failures, which are critical to power transmission and distribution,

represent another category of faults. Additional examples include series faults, where broken lines result in open circuits, and shunt faults, caused by short circuits, which can cascade into wider grid failures. Extreme events, such as hurricanes, lightning strikes, or flashover faults, can damage critical grid infrastructure. Furthermore, the integration of renewable energy sources introduces unique challenges, such as fault currents and the unpredictability of supply from distributed energy resources [31].

Illustrative examples of such faults are depicted in Figure 6a and Figure 6b, which show the time evolution of line frequency during two emblematic catastrophic powerline failures. Figure 6a highlights the blackout that occurred in South Australia on September 28, 2016 [32]. In this case, extreme weather conditions led to the tripping of three transmission lines and initiated a sequence of six faults, resulting in severe frequency instability. Figure 6b captures the blackout on September 8, 2011, which impacted approximately 7 million people across Southern California, Arizona, and parts of Northern Mexico. This event was triggered by interconnected failures during a maintenance operation, causing significant disruptions in power flow. The initial fault led to cascading effects, including voltage and frequency drops, as well as overloads in other parts of the grid [33].

From the analysis of these cases, it is evident that critical faults are often characterized by sudden and significant changes in grid frequency and voltage. These conditions present a substantial challenge for PMUs, which must detect and react to such faults with minimal latency to maintain grid stability and avoid cascading failures.

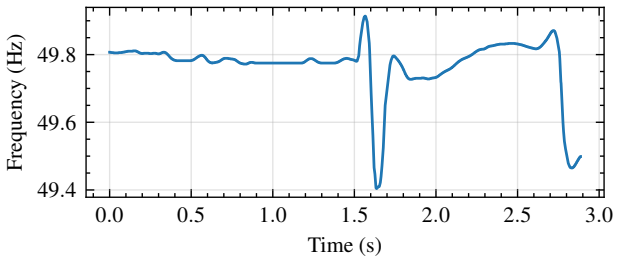

(a) Australia 2016 [32].

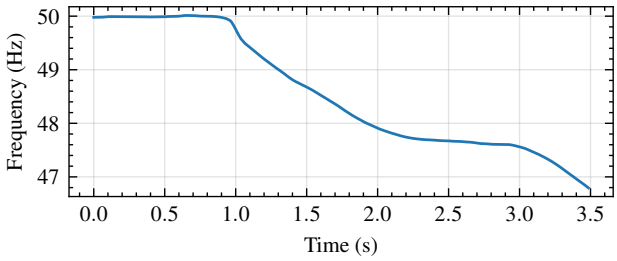

(b) Arizona 2011 [33].

Figure 6. Instantaneous frequency over time. Two case studies: Australia 2016 in (a), Arizona 2011 in (b).

Let us specifically focus on the frequency of the power grid, denoted as $f(t)$, which represents the frequency of the grid at time t. Define t_{S_n} as the time instant when a generic sample n is acquired and transmitted by the PMU, and t_{PDC_n} as the time instant when the sample n is received at the PDC. Let $f(t_{S_n})$ and $f(t_{PDC_n})$ represent the frequency of the power grid at the time of sample acquisition and the frequency at the time of sample reception, respectively.

In general, the difference $t_{PDC_n} - t_{S_n}$ quantifies the transmission latency of the communication system. Under normal operating conditions, we expect the grid frequency to exhibit a quasi-stationary trend, such that $f(t_{PDC_n}) \approx f(t_{S_n})$. In other words, the frequency sampled at t_{S_n} should closely match the grid frequency at t_{PDC_n}, providing an accurate estimation of the current state. Consequently, the frequency estimation error, defined as $E_f = |f(t_{PDC_n}) - f(t_{S_n})|$, is expected to be approximately zero under normal conditions.

A graphical representation of this concept is shown in Figure 7, where circles represent the acquired frequency samples at acquisition times t_{S_n}, and crosses represent the grid frequency at the reception times t_{PDC_n}. Green markers depict normal operation scenarios, where E_f remains close to zero, assuming a transmission latency of 17 ms (taken from the mean value of the simulation with one gNB in Table 2). In contrast, red markers illustrate the sampling process during a fault condition. As shown, under sharp transient conditions, even with the same transmission latency, E_f becomes significantly larger due to the high Rate of Change of Frequency (RoCoF) ($\frac{df}{dt}$). A higher RoCoF implies that, over the span of the transmission latency, the grid frequency undergoes a more substantial change.

This phenomenon is also evident when comparing Figure 7a and Figure 7b. For a given transmission latency, the South Australia case exhibits a noticeably higher E_f than the Arizona case, primarily due to the higher RoCoF during the fault event. In general, the frequency estimation error E_f depends on two major factors: the transmission latency and the RoCoF.

The relationship is straightforward: lower transmission latency and lower RoCoF result in a smaller E_f. Ensuring that E_f remains below a certain threshold is crucial for the proper functioning of distributed PMU systems, especially during fault conditions. In the PDC, these anomalies must be detected and immediately addressed.

Although RoCoF during fault conditions is an intrinsic property of the power grid and cannot be known or controlled a priori, transmission latency is a characteristic of the communication system that can be estimated in advance. This allows predicting the worst-case error E_f during a fault, allowing an assessment of whether the system can react in a timely manner. Therefore, transmission latency emerges as a critical parameter that must be carefully evaluated to ensure the correct operation of PMUs in the presence of faults.

In this context, we evaluated the frequency estimation error under fault conditions for the two case studies discussed above, using the 5G network configuration described in Section 2. to interconnect the PMUs and the PDC. For each case study, we simulated the acquisition and transmission of the faulty frequency profile by one of the UDs (i.e., PMUs) represented in Figure 2. The specific UD tasked with acquiring the faulty sequence was selected randomly, and the faulty profile was randomly shifted within the 900 s simulation time span. This approach ensured comprehensive coverage of diverse network conditions (e.g., initial congestion, steady-state operation, etc.) and various phase shifts of the sampling period.

For each scenario, we conducted 1000 simulations, capturing the worst-case frequency estimation error, E_f, for every instance. This methodology allowed to assess the impact of transmission latency and network dynamics on E_f under fault conditions.

4.1. Simulation results

The simulation results for the two case studies, varying the number of gNBs, are presented in Figure 8 for the Australia 2016 fault and Figure 9 for the Arizona 2011 fault.

Starting with Figure 8, it can be observed that the worst-case frequency estimation error, E_f, exhibits a clear, albeit gradual, decreasing trend as the number of gNBs increases. This trend aligns

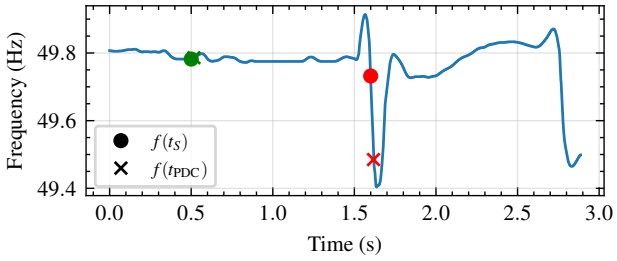

(a) Representation of the error frequency estimation in the case of the Australia 2016 fault.

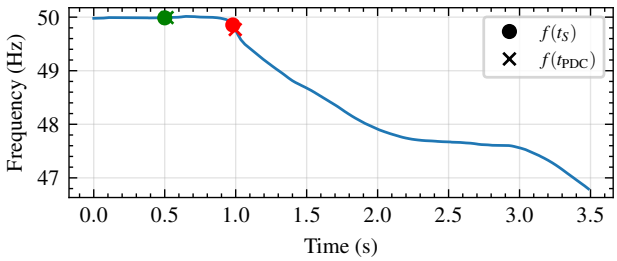

(b) Representation of the error frequency estimation in the case of the Arizona 2011 fault.

Figure 7. Representation of the error frequency estimation in the case of the Australia 2016 fault in (a) and Arizona 2011 in (b).

with the results from the latency and packet loss analysis, confirming the critical role of gNB density in ensuring the reliability and robustness of the communication system. As previously noted, there is a strong relationship between the number of gNBs and latency. Referring to Figure 5, increasing the number of gNBs progressively reduces latency. Consequently, for a fault with a given RoCoF, a higher number of gNBs, and thus lower latency, results in a reduced E_f. Specifically, E_f decreases from approximately 0.24 Hz for scenarios with 1–3 gNBs to around 0.18 Hz for scenarios with more than 7 gNBs.

Special attention should be given to scenarios with 1–3 gNBs, where E_f shows some counterintuitive behavior, particularly in terms of maximum values. It is important to note that this analysis only considers successfully delivered packets. Referring to Table 2, the packet delivery ratio (PDR) is approximately 53% and 94% for configurations with 1 and 2 gNBs, respectively. This indicates a significant number of lost packets. In such cases, the PDC may lose packets corresponding higher RoCoF regions and thus receiving primarily those one corresponding to lower RoCoF regions, artificially reducing E_f. However, as the PDR improves, E_f increases because more samples from regions with higher RoCoF are successfully delivered and processed. This brings up another point that highlights the importance of packet loss in fault detection: packet loss can lead to situations where faults are missed, detected with significant delay, or result in incorrect system state estimation.

Moving to the Arizona 2011 case study, the results shown in Figure 9 reveal a similar trend: E_f decreases with an increasing number of gNBs. However, the dependence on RoCoF is evident. Despite statistically comparable transmission latencies to the Australia 2016 case, the Arizona 2011 case exhibits a consistently lower E_f across all scenarios. For example, E_f ranges from 0.10 Hz for 1–3 gNBs to 0.07 Hz for configurations with 7 or more gNBs. As with the Australia case, the impact of PDR also applies here: higher packet loss can shadow fault conditions or delay their detection, reinforcing the necessity of minimizing packet loss to ensure accurate and timely fault detection.

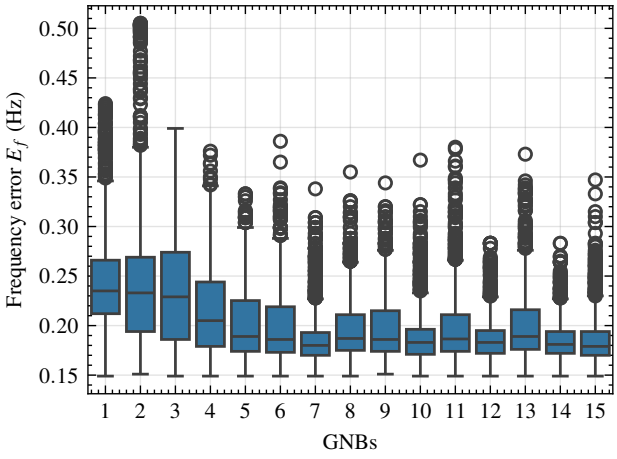

Figure 8. Worst-case frequency estimation error E_f for the Australia 2016 fault.

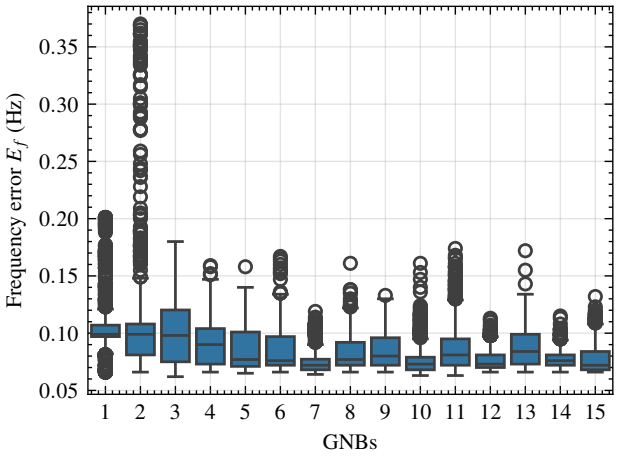

Figure 9. Worst-case frequency estimation error E_f for the Arizona 2011 fault.

4.2. Discussion

First, we emphasize that our analysis focused on faults in frequency profiles. However, the same considerations, without loss of generality, can also be applied to profiles of voltage or current phasor magnitude or phase angle or of other power grid parameters.

The results presented in this section highlight the critical role of 5G communication infrastructure in ensuring the reliability and robustness of PMU-based measurement systems during fault conditions. The ability to detect and respond promptly to grid faults depends on the timely and accurate transmission of data from PMUs to the PDC. As demonstrated, transmission latency, determined by the number of gNBs and network dynamics, plays a crucial role in defining the worst-case frequency estimation error, E_f. Generally, lower latency, achieved through a higher density of gNBs, results in reduced E_f, thereby enhancing the system's fault detection capabilities.

The analysis of the two case studies underscores the importance of considering the specific characteristics of each fault event when designing and deploying PMU-based measurement systems. Faults with higher RoCoF demand lower transmission latencies to keep E_f within acceptable limits. Nonetheless, the obtained results, considering even the case with the highest RoCoF, demonstrate that the 5G network can effectively support fault detection and response in the power grid, achieving response times and E_f values acceptable for a wide range of application scenarios and fault conditions [34]–[36].

Despite these promising results, which are satisfactory for many application scenarios, there remains room for improvement and further mitigation measures. For instance, the adoption of adaptive reporting rate (RR) strategies [11], where PMUs adjust the reporting rate based on grid conditions, could further reduce E_f in fault scenarios. Increasing the reporting rate of a PMU experiencing a fault condition would allow for faster tracking of system dynamics and quicker responses. However, this approach increases network load, which could be mitigated by reducing the reporting rate of other PMUs. Challenges arise when multiple PMUs experience fault conditions simultaneously, potentially overloading the network. To address this, quality of service (QoS) strategies or dedicated bandwidth allocation for fault-affected PMUs could maintain minimal latency even with increased reporting rates. While effective, these solutions introduce additional complexity, operational costs, and system overheads, which must be carefully evaluated for specific application scenarios.

Furthermore, the impact of packet loss on fault detection and response remains a critical area of study. As shown, packet loss can significantly impair fault detection accuracy and timeliness, leading to missed or delayed responses and shadowing the true state of the system. Research such as [37] addresses this challenge by proposing alternative transport techniques and redundancy strategies to mitigate packet loss and enhance communication reliability. However, these enhancements also come with trade-offs in terms of increased system complexity, costs, and in some cases, added latency, necessitating careful evaluation of their applicability to specific scenarios.

Finally, the influence of network dynamics, such as congestion and interference, on fault detection and response requires further exploration. By accounting for these factors, is possible to develop more robust and resilient PMU-based measurement systems capable of real-time fault detection and response, ensuring the stability and reliability of the power grid.

5. CONCLUSIONS

In this paper, we conducted an evaluation of the performance of a 5G infrastructure for transmitting IEC61850 data, particularly focusing on fault-critical conditions in communication systems. In systems reliant on Phasor Measurement Units (PMUs), ensuring low transmission latencies and minimal packet loss is paramount to maintain timeliness in reporting measurements to the Phasor Data Concentrator (PDC) and guarantee system stability. The simulation results show that a 5G infrastructure can effectively serve a PMU-based measurement system. We found that performance in terms of latency and packet loss is strongly influenced by the topology of the 5G network, particularly the number and deployment of gNBs (5G base stations) serving PMUs. Deploying gNBs to serve a limited number of PMUs consistently resulted in low latency and zero packet loss. Using the ultra-low latency profile of 5G, strict deadlines can be set for the PDC to quickly detect synchronization issues, packet loss, and excessive delays.

These results emphasize the critical role of packet delivery reliability in ensuring the robustness of PMU-based systems. Strategies such as adaptive reporting rates and quality-of-service prioritization for fault-affected PMUs offer promising pathways to further improve the system's responsiveness. However, these approaches also introduce trade-offs, such as increased network load and complexity, which need to be carefully managed in real-world applications.

In conclusion, the integration of 5G technologies into PMU-based systems provides significant benefits for fault detection and response in modern power grids. By optimizing network configurations, such as base station density and bandwidth allocation, these systems can achieve the performance required to address the growing challenges of renewable energy integration and grid stability. Future research should focus on refining fault mitigation strategies and exploring scalability to ensure the reliability and resilience of these systems in diverse operational contexts.

Future work will focus on improving the simulation setup by incorporating a more detailed modeling of faults and impairments that affect PMUs and PDCs within the communication network. This will involve simulating various fault scenarios and communication network impairments to better understand their impact on the overall system performance and to mitigation strategies to improve the reliability and resilience of the PMU/PDC system in real-world deployment scenarios.

AUTHORS' CONTRIBUTION

A. Morato led the research and was responsible for all core aspects of the work, including: Conceptualization, Methodology, Software, Validation, Formal analysis, Investigation, Data curation, Visualization, and Writing – original draft.

G. Frigo and F. Tramarin supported the work through Supervision, Funding acquisition, and Writing – review & editing.

All authors have read and agreed to the published version of the manuscript.

REFERENCES

[1] F. Milano, F. Dorfler, G. Hug, D. J. Hill, G. Verbic, Foundations and challenges of low-inertia systems (invited paper), 2018 Power Systems Computation Conference (PSCC), IEEE, Jun. 2018. DOI: 10.23919/pscc.2018.8450880

[2] M. Paolone, T. Gaunt, X. Guillaud, M. Liserre, S. Meliopoulos, A. Monti, T. Van Cutsem, V. Vittal, C. Vournas, Fundamentals of power systems modelling in the presence of converter-interfaced generation, Electric Power Systems Research, vol. 189, Dec. 2020, p. 106811. DOI: 10.1016/j.epsr.2020.106811

[3] R. Hunt, B. Flynn, T. Smith, The substation of the future: Moving toward a digital solution, IEEE Power and Energy Magazine, vol. 17, Jul. 2019, no. 4, pp. 47–55. DOI: 10.1109/mpe.2019.2908122

[4] J. C. Lozano, K. Koneru, N. Ortiz, A. A. Cardenas, Digital substations and iec 61850: A primer, IEEE Communications Magazine, vol. 61, Jun. 2023, no. 6, pp. 28–34. DOI: 10.1109/mcom.001.2200568

[5] Iec international standard - communication networks and systems for power utility automation – all parts, IEC 618502022 SER, 2022, pp. 1–7892. DOI: 10.1109/IEEESTD.2016.7479438

[6] P. Castello, P. Ferrari, A. Flammini, C. Muscas, S. Rinaldi, A new ied with pmu functionalities for electrical substations, IEEE Transactions on Instrumentation and Measurement, vol. 62, Dec. 2013, no. 12, pp. 3209–3217. DOI: 10.1109/tim.2013.2270921

[7] D. D. Giustina, A. Dede, G. Invernizzi, D. P. Valle, F. Franzoni, A. Pegoiani, L. Cremaschini, Smart grid automation based on iec 61850: An experimental characterization, IEEE Transactions on Instrumentation and Measurement, vol. 64, Aug. 2015, no. 8, pp. 2055–2063. DOI: 10.1109/tim.2015.2415131

[8] M. Agustoni, P. Castello, G. Frigo, Phasor measurement unit with digital inputs: Synchronization and interoperability issues, IEEE Transactions on Instrumentation and Measurement, vol. 71, 2022, pp. 1–10. DOI: 10.1109/tim.2022.3175052

[9] Ieee standard for synchrophasor data transfer for power systems, IEEE-C37-118-22011, 2011, pp. 1–7892. DOI: 10.1109/IEEESTD.2016.7479438

[10] M. Asprou, E. Kyriakides, A.-M. Dumitrescu, M. Albu, The impact of pmu measurement delays and a heterogenous communication network on a linear state estimator, 2016 18th Mediterranean Electrotechnical Conference (MELECON), IEEE, Apr. 2016, pp. 1–6.
DOI: 10.1109/melcon.2016.7495338

[11] G. Frigo, P. A. Pegoraro, S. Toscani, Tracking power system events with accuracy-based pmu adaptive reporting rate, International Journal of Electrical Power & Energy Systems, vol. 153, 2023, p. 109384.

[12] A. Taik, B. Nour, S. Cherkaoui, Empowering prosumer communities in smart grid with wireless communications and federated edge learning, IEEE Wireless Communications, vol. 28, Dec. 2021, no. 6, pp. 26–33.
DOI: 10.1109/mwc.017.2100187

[13] M. H. Rehmani, M. Reisslein, A. Rachedi, M. Erol-Kantarci, M. Radenkovic, Integrating renewable energy resources into the smart grid: Recent developments in information and communication technologies, IEEE Transactions on Industrial Informatics, vol. 14, Jul. 2018, no. 7, pp. 2814–2825.
DOI: 10.1109/tii.2018.2819169

[14] V.-G. Nguyen, K.-J. Grinnemo, J. Taheri, A. Brunstrom, A deployable containerized 5g core solution for time critical communication in smart grid, 2020 23rd Conference on Innovation in Clouds, Internet and Networks and Workshops (ICIN), IEEE, Feb. 2020.
DOI: 10.1109/icin48450.2020.9059397

[15] D. Carrillo, C. Kalalas, P. Raussi, D. S. Michalopoulos, D. Z. Rodríguez, H. Kokkoniemi-Tarkkanen, K. Ahola, P. H. Nardelli, G. Fraidenraich, P. Popovski, Boosting 5g on smart grid communication: A smart ran slicing approach, IEEE Wireless Communications, vol. 30, Oct. 2023, no. 5, pp. 170–178.
DOI: 10.1109/mwc.004.2200079

[16] F. Lamonaca, D. L. Carnì, Evaluation of the Effects of Mobile Smart Object to Boost IoT Network Synchronization, Sensors, vol. 21, Jan. 2021, no. 12, p. 3957.
DOI: 10.3390/s21123957

[17] N. Veerakumar, D. Ćetenović, K. Kongurai, M. Popov, A. Jongepier, V. Terzija, Pmu-based real-time distribution system state estimation considering anomaly detection, discrimination and identification, International Journal of Electrical Power & Energy Systems, vol. 148, 2023, p. 108916.

[18] G. I. Karvelis, G. N. Korres, O. A. Darmis, State estimation using scada and pmu measurements for networks containing classic hvdc links, Electric Power Systems Research, vol. 212, 2022, p. 108544.

[19] Q. Zhang, Y. Chakhchoukh, V. Vittal, G. T. Heydt, N. Logic, S. Sturgill, Impact of pmu measurement buffer length on state estimation and its optimization, IEEE Transactions on Power Systems, vol. 28, 2012, no. 2, pp. 1657–1665.

[20] S. M. Blair, M. H. Syed, A. J. Roscoe, G. M. Burt, J.-P. Braun, Measurement and analysis of pmu reporting latency for smart grid protection and control applications, IEEE Access, vol. 7, 2019, pp. 48 689–48 698.

[21] B. Appasani, D. K. Mohanta, A review on synchrophasor communication system: communication technologies, standards and applications, Protection and control of modern power systems, vol. 3, 2018, no. 4, pp. 1–17.

[22] K. Narendra, T. Weekes, Phasor measurement unit (pmu) communication experience in a utility environment, conference on power systems, 2008, vol. 21.

[23] A. Morato, G. Frigo, F. Tramarin, Fault simulation in Phasor Measurement Units: A study on system reaction time in a 5G network environment, Measurement: Sensors, Dec. 2024, p. 101445.
DOI: 10.1016/j.measen.2024.101445

[24] I. Ahmed, E. Balestrieri, P. Daponte, R. Imperatore, F. Lamonaca, M. Paolucci, F. Picariello, Morphometric Measurement of Fish Blood Cell: An Image Processing and Ellipse Fitting Technique, IEEE Transactions on Instrumentation and Measurement, vol. 73, 2024, pp. 1–12.
DOI: 10.1109/TIM.2024.3353280

[25] A. Derviskadic, P. Romano, M. Pignati, M. Paolone, Architecture and experimental validation of a low-latency phasor data concentrator, IEEE Transactions on Smart Grid, vol. 9, Jul. 2018, no. 4, pp. 2885–2893.
DOI: 10.1109/tsg.2016.2622725

[26] A. Derviskadic, P. Romano, C. Get, W. Koong Chai, C. Develder, L. Zanni, M. Pignati, M. Paolone, Design and experimental validation of an lte-based synchrophasor network in a medium voltage distribution grid, 2018 Power Systems Computation Conference (PSCC), IEEE, Jun. 2018, pp. 1–7.
DOI: 10.23919/pscc.2018.8442644

[27] Omnet++ official webpage, https://omnetpp.org/, accessed December 30, 2024.

[28] Simu5g official website, http://simu5g.org/, [Online; accessed December 30, 2024].

[29] G. Nardini, D. Sabella, G. Stea, P. Thakkar, A. Virdis, Simu5g–an omnet++ library for end-to-end performance evaluation of 5g networks, IEEE Access, vol. 8, 2020, pp. 181 176–181 191.
DOI: 10.1109/access.2020.3028550

[30] A. F. Gentile, D. Macrì, D. L. Carnì, E. Greco, F. Lamonaca, A Performance Analysis of Security Protocols for Distributed Measurement Systems Based on Internet of Things with Constrained Hardware and Open Source Infrastructures, Sensors, vol. 24, Jan. 2024, no. 9, p. 2781.
DOI: 10.3390/s24092781

[31] Z. Krivohlava, S. Chren, B. Rossi, Failure and fault classification for smart grids, Energy Informatics, vol. 5, Oct. 2022, no. 1, p. 33.
DOI: 10.1186/s42162-022-00218-3

[32] Review of the System Black Event in South Australia on 28 September 2016 | AEMC. Online. [Accessed: 14 January 2025].
https://www.aemc.gov.au/markets-reviews-advice/review-of-the-system-black-event-in-south-australi

[33] September 2011 Southwest Blackout Event. Online. [Accessed: 14 January 2025].
https://www.nerc.com/pa/rrm/ea/pages/september-2011-southwest-blackout-event.aspx

[34] X. Qi, M. Wen, X. Yin, Z. Zhang, J. Tang, F. Cai, A novel fast distance relay for series compensated transmission lines, International Journal of Electrical Power & Energy Systems, vol. 64, Jan. 2015, pp. 1–8.
DOI: 10.1016/j.ijepes.2014.07.028

[35] S. P. Valsan, K. S. Swarup, High-Speed Fault Classification in Power Lines: Theory and FPGA-Based Implementation, IEEE Transactions on Industrial Electronics, vol. 56, May 2009, no. 5, pp. 1793–1800.
DOI: 10.1109/TIE.2008.2011055

[36] S. Zarbita, A. Lachouri, H. Boukadoum, A new approach of fast fault detection in HV-B transmission lines based on Detail Spectrum Energy analysis using oscillographic data, International Journal of Electrical Power & Energy Systems, vol. 73, Dec. 2015, pp. 568–575.
DOI: 10.1016/j.ijepes.2015.05.047

[37] A. Morato, G. Frigo, F. Tramarin, 5G-Enabled PMU-Based Distributed Measurement Systems: Network Infrastructure Optimization and Scalability Analysis, IEEE Transactions on Instrumentation and Measurement, vol. 73, 2024, pp. 1–12.
DOI: 10.1109/TIM.2024.3457959